Finding Adhesion Energies of Graphene and MoS_2 to Determine Optimal 2D Electron Transport for Thermo-Electric Power Conversion Devices

Jorge Torres, Yisi Zhu, Pei Liu, Seong Chu Lim, Seth So, and Minhee Yun

PITT | SWANSON ENGINEERING

Mascaro Center for Sustainable Innovation

Introduction

2-Dimensional materials have uniquely high electrical and thermodynamic conductivities due to their high surface area to volume ratios. This property can be utilized in thermoelectric power devices to efficiently capture the electron flow of heat gradients and convert it into harvestable energy.

However, integration of 2D materials with devices can be difficult due to small sizing and directional fragility. While 2D materials can be grown or deposited without issue, they often need to undergo a wet transfer process to be used in micro-electronics. This transfer process can significantly affect the properties of 2D materials and must be investigated.

In this research, 2D MoS_2 and Graphene were investigated to determine the adhesion energies of each on different metal substrates. Doing so would help to inform the design of the devices and lend practical considerations for fabrication and testing.

Sample Preparation

1. Growth substrate for 2D material is chosen and prepared
2. 2D material is grown onto substrate via CVD methods
3. PMMA is spun onto sample after excess material is removed
4. Sample is placed into etchant bath to remove substrate
5. PMMA – 2D material hybrid is cleaned acetone and IPA
6. Metal adhesion substrate is chosen and prepared
7. Gold nanoparticle solution is deposited and dried on substrate
8. 2D material is transferred on top of substrate, forming a nanoparticle blister

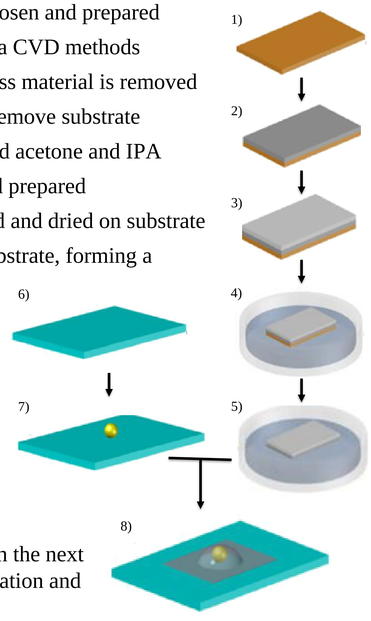

The adhesion energy is calculated from sample measurements taken from AFM imaging. The physical parameters of blister size are indicative of how tightly the 2D material adheres around the gold nanoparticle, which in turn can be extrapolated to adhesion energy through various modeling.

Parameters and equations are described in the next section. Calculations assume that deformation and contact area is negligible.

Calculations

Calculations were made according to prior work done by Wan et al. The blister was modeled as a thin, flexible membrane with an external central load (nanoparticle). Defining elastic response yielded:

$$\frac{d}{dr}\left(\nabla^2 f\right) + \frac{Eh}{r}\left(\frac{dw}{dr}\right)^2 = 0 \quad , \quad [E] \text{ - Young's Modulus} \qquad (1)$$

This helped establish a load function, which gave an energy balance equation for an elastic system at equilibrium. In present context, interfacial energy γ is:

$$\gamma = \lambda Eh\left(\frac{w}{a}\right)^4 \quad , \quad \lambda = 1/16 \qquad (2)$$

Other assumptions include a small debonding angle and spherical shape.

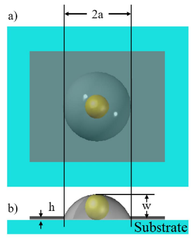

Figure 1. Physical representation of parameters in equation (2). a) top view; b) cross-sectional view

AFM Imaging

First, simple blisters were identified using SEM (Zeiss Sigma 500 VP). Figure 2 below shows a sample of Graphene on SiN and the different blisters that formed on each sample. Position A is the desired simple blister, with no wrinkling. Position B shows a compound blister of many nanoparticles that formed as a result of clumping as during evaporation. Position C displays a single nanoparticle blister, but the graphene layer on top has a wrinkle. Position A is the measurement target, as the modelling process makes several assumptions that are only justified in the simplest case.

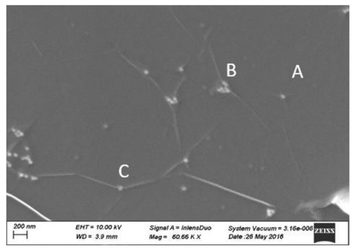

Figure 2. SEM image of graphene on SiN with gold nanoparticles. Working distance: 3.9mm, Magnification: 60.66kx, electron beam: 10kV.

After identification, an AFM was used for sample measurement. The AFM was set to tapping mode in a 500μm x 500μm scanning area around the blister, with 400 x 400 pixel resolution. AFM software allowed for blister height (w) and blister diameter (2a) to be accurately measured. The samples consisted of Graphene and MoS_2 2D layers each on top of SiO_2, SiN, Au, and Pt metal substrates with gold nanoparticles deposited on top.

Figure 3 below shows the AFM images of several samples with corresponding raw data visualization. Brighter areas represent larger height measurements, and the graphed data provides a cross-sectional representation of the blister, with direction of scan displayed on the image.

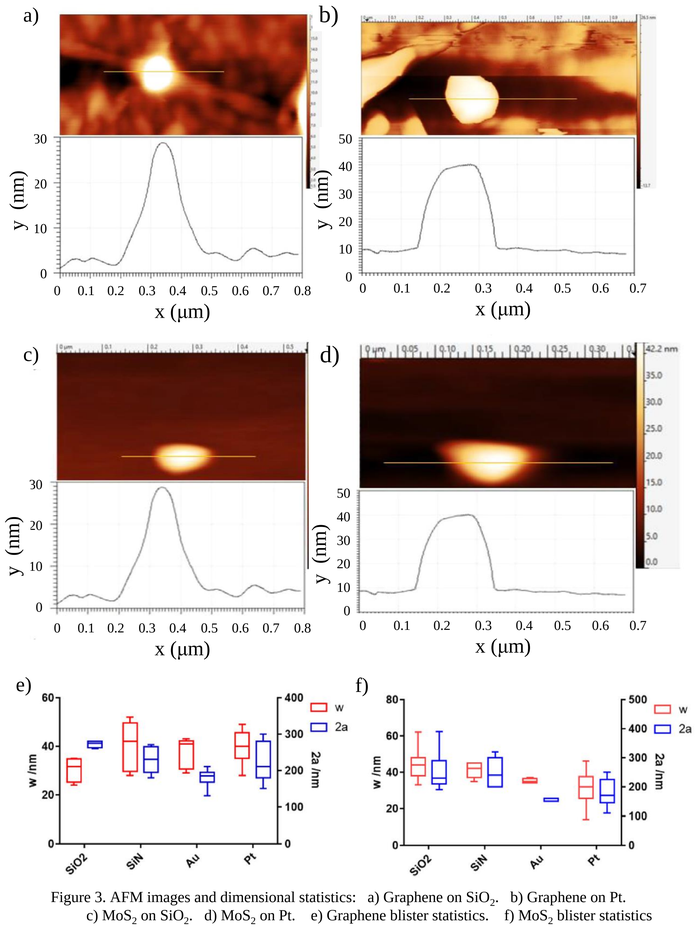

Figure 3. AFM images and dimensional statistics: a) Graphene on SiO_2. b) Graphene on Pt. c) MoS_2 on SiO_2. d) MoS_2 on Pt. e) Graphene blister statistics. f) MoS_2 blister statistics

The AFM was able to measure each sample surface and provide relative views of each substrate. Metal substrates were easily comparable by looking at the cross-section data, which itself gives insight into the adhesion energies before calculation.

Adhesion Energies

Adhesion energies of each sample were calculated (E_{grn} = 1TPa, E_{MoS2} = 0.33TPa) using (2) and averaged to produce the results in table 1:

Substrate	Graphene [mJ m^{-2}]	MoS_2 [mJ m^{-2}]
SiO_2	567.14	482.48
SiN	3281.64	429.00
Au thin film	7687.10	1207.26
Pt thin film	4021.47	690.64

Table 1. Experimental adhesion energies of Graphene and MoS_2 to SiO_2, SiN, Au, and Pt metal substrates

Graphene showed overall stronger bonding to substrates than MoS_2, and both 2D materials had significantly better adhesion to gold than to other metals. This may be due to other forces not expressed in (2), such as Van der Waals, as Au is the most polarizing of the substrates.

Conclusion and Future Work

In this research, the adhesion energies of Graphene and MoS_2 were successfully determined utilizing a nanoparticle intercalation method involving AFM measurements and thin membrane calculations. Graphene would likely perform more reliably than MoS_2 because of its higher adhesion energies; graphene will be able to maintain better contact and hence better conduction. This is in part due to graphene's extraordinarily high Young's modulus, and confirms that there is a direct relation between Young's modulus $E_{material}$ and interfacial/adhesion energy γ. However, results also suggest that this difference may be overcome by other factors such as polarization factor.

Results suggest that a graphene bridge be used and anchored with gold contacts for TEP devices for optimal transfer efficiency and structural security. Future work involves further characterizing thin film electrical and thermal conductivity, bridge resistance, and overall device efficacy.

Acknowledgements

The Mascaro Institute for Sustainable Innovation for summer funding.

The authors are grateful for financial support from the National Science Foundation (NSF), ECCS 1709307 and from NSF HRD 1434012.

Contact information: miy16@pitt.edu

References

[1] A. Gupta, T. Sakthivel, S. Seal, Prog. Mater. Sci. 2015, 73, 44. **[2]** A. C. Ferrari, F. Bonaccorso, V. Fal'Ko, K. S. Novoselov, S. Roche, P.Bøggild, S.Borini,F.H.Koppens, V.Palermo,N.Pugno, J.A.Garrido, Nanoscale 2015, 7, 4598. **[3]** Z. Guo, R. Dong, P. S. Chakraborty, N. Lourenco, J. Palmer, Y. Hu, M. Ruan, J. Hankinson, J. Kunc, J. D. Cressler, C. Berger, Nano Lett. 2013, 13.3, 942. **[4]** A. Urich, K. Unterrainer, T. Mueller, Nano Lett. 2011, 11.7, 2804. **[5]** E. J. Yoo, J. Kim, E. Hosono, H. Zhou, T. Kudo, I. Honma, Nano Lett. 2008, 8.8, 2277. **[6]** H. Kurokawa, J. Electrochem. Soc. 1982, 129.11, 2620. **[7]** S. Das, D. Lahiri, D. Y. Lee, A. Agarwal, W. Choi, Carbon 2013, 59, 121. **[8]** C. Gong, L. Colombo, R. M. Wallace, K. Cho, Nano Lett. 2014, 14, 1714. **[9]** S. Fratini, F. Guinea, Phys. Rev. B. 2008, 77, 195415. **[10]** S. Y. Zhou, G. H. Gweon, A. V. Fedorov, P. N. First, W. A. De Heer, D. H. Lee, F. Guinea, A. C. Neto, A. Lanzara, Nat. Mater. 2007, 6, 770. **[11]** Z. Lu, M. L. Dunn, J. Appl. Phys. 2010, 107.4, 044301. **[12]** T. Yoon, W. C. Shin, T. Y. Kim, J. H. Mun, T. S. Kim, B. J. Cho, Nano Lett. 2012, 12.3, 1448. **[13]** Y. Li, M. Li, T. Wang, F. Bai, Y. X. Yu, Phys. Chem. Chem. Phys. 2014, 16, 5213. **[14]** S. P. Koenig, N. G. Boddeti, M. L. Dunn, J. S. Bunch, Nat. Nanotechnol. 2011, 6.9, 543. **[15]** Z. Zong, C. L. Chen, M. R. Dokmeci, K. Wan, J. Appl. Phys. 2010, 107.2, 026104. **[16]** G. H. Han, N. J. Kybert, C. H. Naylor, B. S. Lee, J. Ping, J. H. Park, J. Kang, S. Y. Lee, Y. H. Lee, R. Agarwal, A. C. Johnson, Nat. Commun. 2015, 6, 6128. **[17]** K. T. Wan, Y. W. Mai, Int. J. Fract. 1996, 74.2, 181. **[18]** Z. Cao, P. Wang, W. Gao, L. Tao, J. W. Suk, R. S. Ruoff, D. Akinwande, R. Huang, K. M. Liechti, Carbon 2014, 69, 390. **[19]** A. Castellanos-Gomez, M. Poot, G. A. Steele, H. S. van der Zant, N. Agraït, G. Rubio-Bollinger, Adv. Mater. (Weinheim, Ger.) 2012, 24.6, 772. **[20]** J. S. Bunch, M. L. Dunn, Solid State Commun. 2012, 152.15, 1359. **[21]** X. Zhang, Z. Gong, J. Li, T. Lu, J. Chem. Inf. Model. 2015, 55, 2138. **[22]** J. N. Israelachvili, Intermolecular and Surface Forces, Elsevier Academic, Amsterdam, NL 2011.